

# Application of Chemo-Rheology to Establish a Process Window for a New Solventless System to Manufacture Pre-pregs and Laminates for Electronic Applications

L. M. DEHNKE, PERMADI, J. M. CASTRO

Department of Industrial and Systems Engineering, The Ohio State University, Columbus, Ohio 43210

Received 30 August 2000; revised 6 January 2001; accepted 25 January 2001

**ABSTRACT:** The most common commercial processes for manufacturing pre-pregs for electronic applications use solvent-based epoxy systems. Solvents are environmentally unfriendly and contribute to voids in the pre-preg and laminate. Voids cause product variability, which is a major source of scrap in board shops. In this paper, we use chemo-rheological and kinetic measurements to identify a potential epoxy-based resin system for a solventless process that is based on injection pultrusion. Differential scanning calorimetry and rheological data show that the candidate system does not react appreciably without catalyst up to temperatures of 170 °C or with catalyst at temperatures <110 °C. The system solidifies at temperatures <105 °C. The overall viscosity of the resin system is dependent on the temperature, degree of cure, and filler content. Kinetic rate and viscosity rise expressions to be used in process modeling and optimization have been developed. A preliminary process window for the process is established. © 2001 John Wiley & Sons, Inc. *J Appl Polym Sci* 82: 601–610, 2001

**Key words:** solventless lamination; pre-preg; rheology; process window; kinetic rate

## INTRODUCTION

Printed circuit boards (PCBs) are the foundation of virtually all electronic products. They are the platform on which electronic components are mounted and interconnected. The substrates used for fabricating PCBs are commonly known as copper-clad laminates. Laminates are usually made from organic laminated materials consisting of a particular resin, usually an epoxy or phenolic, embedded with some type of reinforcement, either glass or paper, and with copper foil attached to the outer surfaces.

In addition to being environmentally detrimental, the current process of lamination has several

drawbacks that cause product variability. The first step in the conventional lamination process, as seen in Figure 1, is the impregnation of an epoxy resin mixture into a glass fiber reinforcement layer. The epoxy is dissolved in a solvent, typically acetone or dimethylformamide (DMF). The solvent is used to lower the viscosity and to dissolve the catalyst in the epoxy system. Many of the solvents used are regulated substances.<sup>1</sup> Great care must be given to their use, recovery, and disposal. The glass fabric is secured by sets of rollers that pass it through the resin dip pan, where excess resin is removed, and then into a heating chamber called a treater, where the glass fabric is dried and the resin is partially cured. Because impregnation is carried out at low pressures, cylindrical voids, often referred to as cigar voids, are usually present within the fiber tows.<sup>2</sup> If the resin mat is dried too quickly in the heating

---

Correspondence to: J.M. Castro (castro.38@osu.edu).

*Journal of Applied Polymer Science*, Vol. 82, 601–610 (2001)  
© 2001 John Wiley & Sons, Inc.

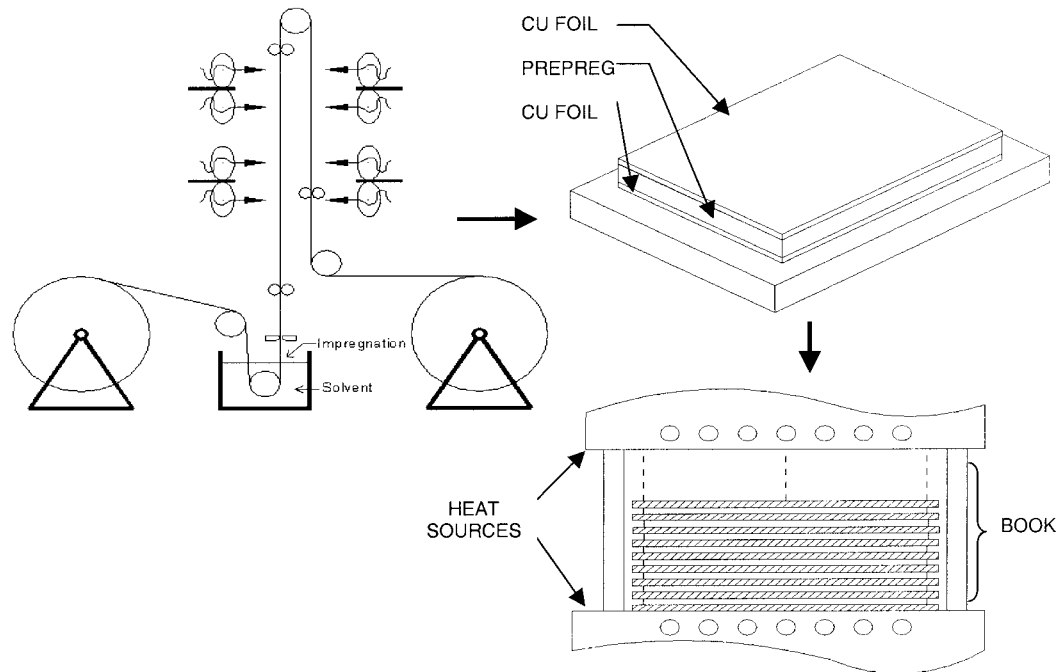


**Figure 1** Schematic representation of conventional lamination process.

chamber, the evaporating solvent will boil and leave spherical voids.<sup>3</sup> Voids contribute to variability between different rolls of pre-preg. This variability is a major source of scrap at board shops.<sup>4</sup>

The pre-preg can be sold directly to customers or undergo further processing to create a copper-clad laminate, in which case it would be referred to as b-stage. Depending on the design requirements, the laminate is constructed from copper foil and multiple layers of b-stage. As seen in Figure 1, the b-stage is stacked to form a book of laminates with stainless steel inserts and Kraft paper press pads on both sides of the book. The stainless steel serves as a separator between adjacent laminates, whereas the Kraft paper is both a thermal and mechanical damper to produce a more uniform temperature distribution across the book surfaces. The books are placed in the heating cavity for a given cure cycle consisting of varying pressures and temperatures depending on the type of b-stage. According to its position in the book, the cure/thermal history of a laminate will vary. A laminate near the edge of the book will cure faster than one in the center. So, within a single book, there will be differences in the residual stresses from one laminate to another. These differences are a source of product variability.

The drawbacks of the conventional lamination processes can be summarized into three main ar-

eas. First, solvents are hazardous to employees as well as the environment. Second, voids, whether they are caused by incomplete impregnation or by solvent boiling, not only contribute to pre-preg variability but also to electrical shorts. If a drilled hole penetrates a void, the copper solution used to plate the hole may migrate into the void and create a short between a plated through hole and a circuit layer not connected to that hole, causing circuit board failure.<sup>5</sup> Third, the unequal cure/temperature histories in the book bring inconsistencies to the laminates. Inconsistencies in the laminates and, in particular, in the pre-preg, as already mentioned, are one of the major causes scrap in a board shop.<sup>4</sup>

To eliminate these drawbacks, a continuous solventless approach to laminate production is being developed in our laboratory. A solventless system would eliminate the costs and regulatory demands of handling, storing, and disposing of solvents. The manufacture of laminates would be less harmful to employees and the environment. If solvents are no longer in the system, their ill effects on laminate quality will also disappear. Figure 2 is a schematic representation of our solventless approach to continuous lamination. Instead of dipping the reinforcing material into a resin and solvent bath in an open pan, the glass fabric will be impregnated with the use of a die. Similar to the concept of injection pultrusion, the

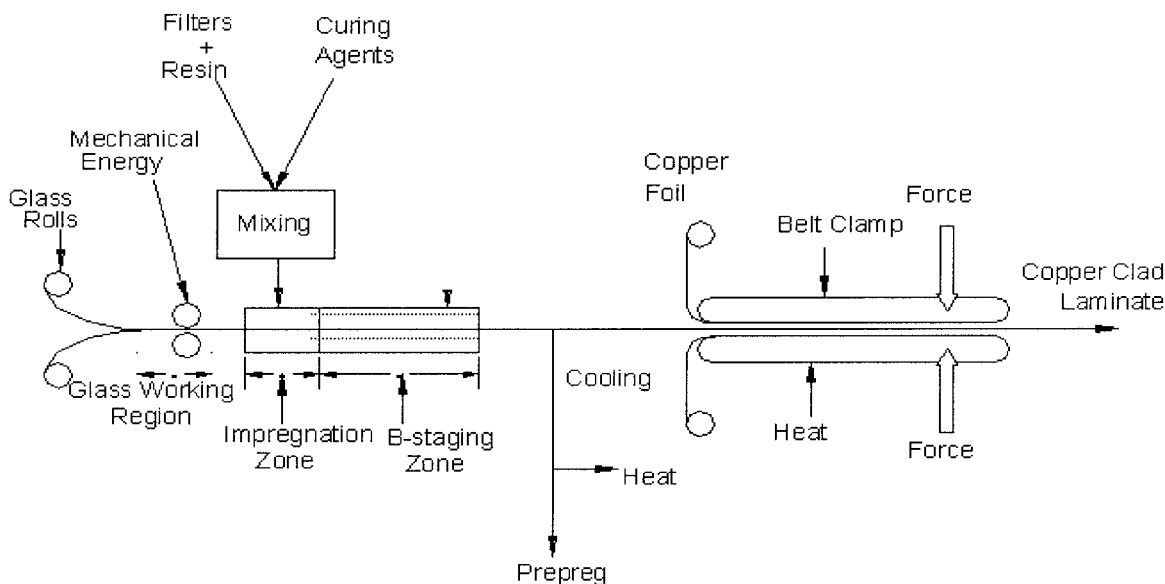


Figure 2 Solventless approach to continuous lamination.

fabric will be impregnated with resin as it passes through the die.<sup>6, 7</sup> Depending on the material chemo-rheology, as will be discussed later, the material can be b-staged in the die or in a subsequent oven or in a combination of both. In this way, the occurrence of voids in the pre-preg caused by low-pressure application and solvent boiling will be eliminated. In this continuous process, the b-stage material can be made into a laminate or removed from the process to be sold as pre-preg. When producing pre-preg, the material will have to be cooled below its solidification temperature prior to the pulling mechanism. Because the final cure and pressing are done in a continuous lamination belt clamp, the variability in cure/temperature histories from one laminate to another are eliminated.

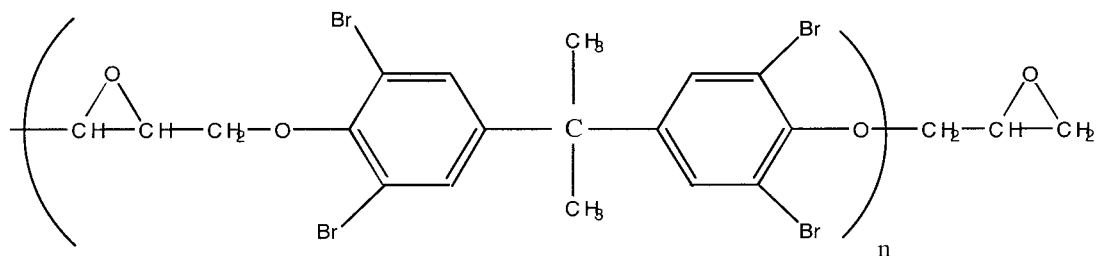
There are several factors that must be considered for the proposed solventless process to be successful. First, a suitable resin needs to be identified. The resin system and catalyst need to be miscible without the use of a solvent. The chemo-rheology of the system needs to be such that its initial viscosity is low enough to permit adequate impregnation. The viscosity must allow the pulling force to be low enough to avoid distorting the mat at a pulling speed fast enough to compete with the current processes. The curing rate should be fast enough so that the residence time required in the b-staging zone and lamination clamp are such that required lengths of these areas are reasonable.

In this paper we describe the application of chemo-rheological measurements to identify a suitable resin system and to develop a process window for the solventless system. Kinetic rate expressions based on Kamal's autocatalytic model<sup>8</sup> are obtained. An equation describing the chemo-rheology of the system is developed. These expressions can be used to model and optimize the process.

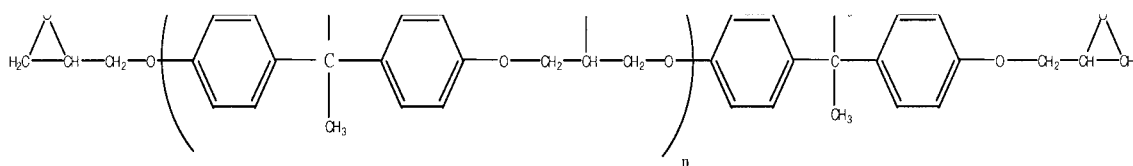
## EXPERIMENTAL

Electronic type epoxy resin formulations consist of several key components. The epoxy resin is mixed with a curing agent of some kind. The curing agent is very important in that it directly affects the type of network formed in the cured polymer.<sup>3</sup> To make a laminate, some kind of fiber reinforcement is required to support the polymer matrix. Other components may include accelerators or fillers. Accelerators tend to act as catalysts by lowering the activation energy of the reaction. Fillers can be added to enhance the properties of the finished product. For example, fused silica reduces the dielectric loss of the finished laminate.

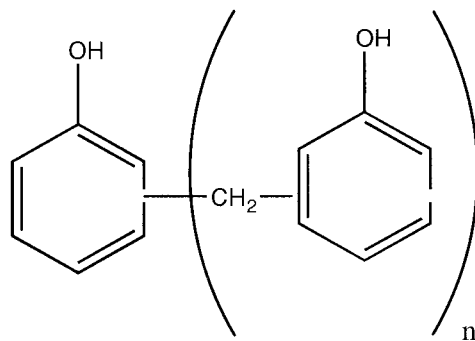
A common epoxy resin used in traditional printed circuit board fabrication is the diglycidyl ether of bisphenol A (DGEBA). A commonly used catalyst is 2-methyl-imidazole (2-MI), which cannot be used in a solventless system because it is



DER 542, epichlorohydrin and tetrabromobisphenol A



DER 383, epichlorohydrin and bisphenol A



SD-1731, phenolic novolak

**Figure 3** Chemical formulae of candidate system components.

not soluble in the epoxy without solvent. We used 2,4-ethyl-methyl-imidazole (2,4-EMI) instead because it is soluble in DGEBA-based epoxies without the use of solvent. Discussions with Dow Chemical Corporation resulted in an initial candidate system consisting of DER 383 (non-brominated DGEBA) and DER 542 (brominated DGEBA). One of the long-term goals of the project is to develop not only a solventless system, but also obtain V-0 flammability without using a brominated resin. Therefore, we included a phenolic novolak-based resin (SD-1731) as the third resin

component to gain the required fire retardancy. The generic chemical formulas are given in Figure 3, as best ascertained from the Material Safety Data Sheets.

The ideal formulation will have a low enough viscosity to facilitate impregnation and minimize the pulling force and cure in a reasonable time. Chemo-rheological testing was used to screen for a potential resin mixture. The mixture suggested as a starting point by Dow Chemical is 52 parts DER 542, 48 parts DER 383, and 40 parts SD-1731. Experiments were done with 0.05 and 0.1%

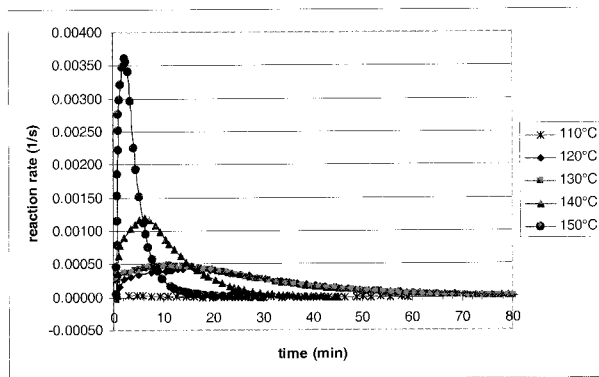


**Figure 4** Isothermal reaction rate at several temperatures.

catalyst levels by weight, and fused silica was added at levels of 10, 20, and 40% by weight.

## RESULTS AND DISCUSSION

### Kinetics

To develop a kinetic rate expression for the resin system, differential scanning calorimetry (DSC) was used. The basic assumption in DSC kinetic measurements is that the rate of heat generation is proportional to the rate of the cure reactions.<sup>9</sup> The rate at which heat is provided to the sample,  $dh_s/dt$ , is equivalent to the rate of increase of internal energy minus the rate of heat production by the reaction:

$$dh_s/dt = mC_p dT/dt - dh_r/dt \quad (1)$$

for isothermal conditions ( $dT/dt = 0$ ). The fraction of heat evolved by the reaction at a certain time is equal to the reactive group conversion,  $c^*$ :

$$c^*(t) = \frac{\int_0^t (mC_p dT/dt - dh_s/dt) dt}{\int_0^\infty (mC_p dT/dt - dh_s/dt) dt} = \frac{a(t)}{A} \quad (2)$$

where  $c^*$  is the reactive group conversion,  $m$  the sample mass,  $C_p$  is the heat capacity, and  $T$  is the sample temperature. The heat of reaction is given by

$$\Delta H = A/m \quad (3)$$

where  $m$  is the mass of the sample.

Isothermal DSC runs for the candidate resin mixture with 0.05% catalyst by weight were carried out at 110, 115, 120, 130, 140, and 150 °C. The reaction rates versus time for these runs are shown in Figure 4. The run at 115 °C was not included for clarity, because it was very close to the reaction rate displayed at 120 °C. The isothermal runs were concluded when there was no further heat evolved. At 110 °C, negligible reaction occurred within the time scale of the experiment, which was 60 min.<sup>2</sup> The residual heat was determined by following the isothermal run with a dynamic scan at 5 °C/min from 50 to 240 °C. A second scan was done to measure the glass transition temperature ( $T_g$ ). The total heat of reaction was calculated as the sum of the heat evolved during the isothermal reaction and the residual heat. The isothermal run at 150 °C did not display any residual heat in the dynamic scan following the isotherm. The total heats of reaction at the different temperatures are shown in Figure 5. For comparison, a dashed line shows the total heat evolved from the dynamic scan of a fresh mixture, which is 265 J/g. It was assumed that the isothermal runs at 140 and 150 °C lost some heat before the DSC was able to record it. The amount of energy lost was assumed to be equal to the difference with the dynamic scan. However, the lower total heat shown for the 115 and 120 °C runs is most likely indicative of a different reaction dominating at lower temperatures. This suggestion is supported by the lower  $T_g$  values shown in Figure 6. This figure shows about the same  $T_g$  as obtained for the fresh mixture after a dynamic scan

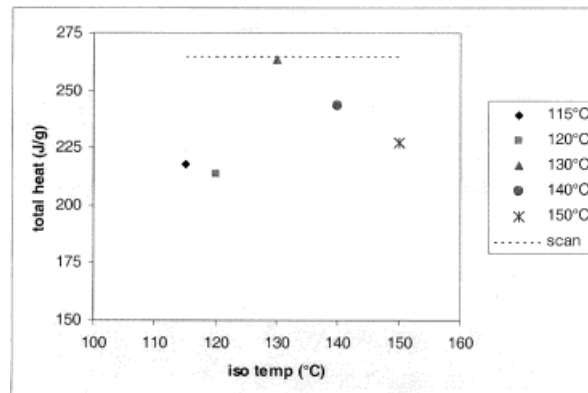


**Figure 5** Total heat from isothermal runs compared with dynamic scan.

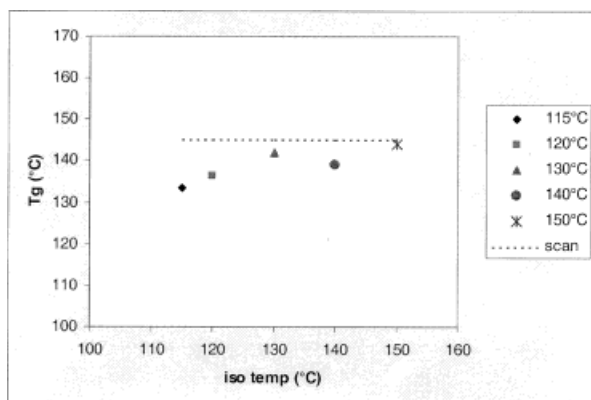


**Figure 6** Final  $T_g$  of isothermal runs compared with dynamic scan.

if the reaction temperature is 130 °C or larger (again shown as a dashed line).

Using the data, kinetic parameters were obtained for the phenomenological autocatalytic model proposed by Kamal and Sorour<sup>8</sup> as seen in eqs. 4–6. The constants obtained for the model are seen in Table I.<sup>2</sup>

$$\frac{dc^*}{dt} = (k_1 + k_2 c^{*m})(c_{\text{inf}} - c^*)^n \quad (4)$$

$$k_1 = k_{01} \exp(-E_1/RT) \quad (5)$$

$$k_2 = k_{02} \exp(-E_2/RT) \quad (6)$$

Two sets of constants are obtained for the 0.05% catalyst level, one is valid for temperatures <130 °C and the other for temperature of  $\geq 130$  °C. The predictions of the model are compared with experimental results in Figure 7 for the isothermal runs at 130, 140, and 150 °C. Two sets of experimental runs are shown at each temperature. The

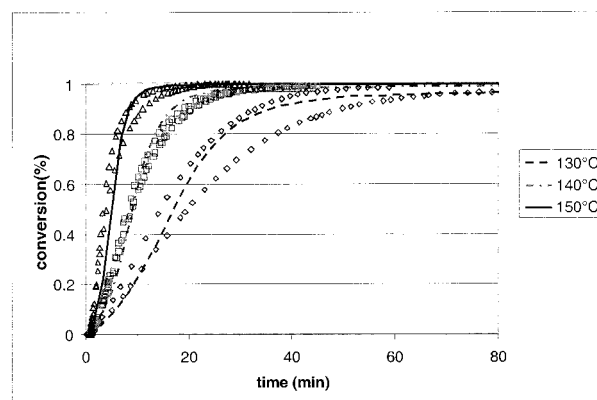


**Figure 7** Predicted fit (solid lines) to experimental isothermal data (open symbols).

repeatability of the data is typical of reactive processing when commercial materials are used. The model does a reasonable job predicting the reaction profiles. For the 0.1% catalyst level, the kinetic parameters were obtained by using only the dynamic scan shown in Figure 8. The dynamic scan for 0.05% catalyst is shown for comparison. A comparison of the predicted reaction profiles for the dynamic scan for both catalyst levels is shown in Figure 9. The values for 0.1% catalyst should be valid for the higher temperature regime. No isothermal scans were carried out at the 0.1% catalyst level because at this stage we were only interested on a relative comparison with the 0.05% level.

### Chemo-rheology

Viscosity is the most important material property in polymer processing operations involving flow.<sup>10</sup> In the case of reactive systems, we need to obtain the change in viscosity with chemical reaction. The kinetic expressions presented in the previous

**Table I** Autocatalytic Model Constants Used in Analysis<sup>a</sup>

Constant	Region		
	115–130°C 0.05% Catalyst	Above 130°C 0.05% Catalyst	Above 130°C 0.1% Catalyst
$k_{01}$ (s <sup>-1</sup> )	0.485	35	35
$k_{02}$ (s <sup>-1</sup> )	$1.93 \times 10^{-3}$	$8.0 \times 10^{11}$	$8.0 \times 10^{11}$
$E_1$ (KJ/mol)	26.43	40	37
$E_2$ (KJ/mol)	0.506	111	111

<sup>a</sup> Reference 2

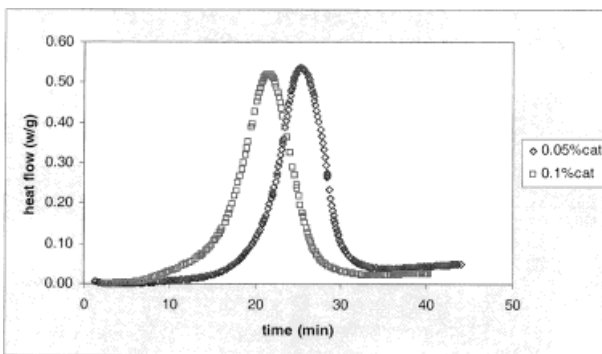


**Figure 8** DSC scans of the two catalyst levels tested.

section were used to map viscosity versus reaction time to viscosity versus extent of reaction. The viscosity of reactive systems is affected by temperature, extent of reaction, filler concentration, if present, and, in some cases, by shear rate. All viscosity measurements reported were obtained with a Rheometrics RMS 800 rheometer, using the parallel plate fixture.

As previously discussed, the mixture does not react appreciably even with catalyst at temperatures  $<110$  °C. To keep the mixture a liquid, the temperature needs to be  $>105$  °C. DSC measurements also indicated that the mixture did not react appreciably at any temperature without catalyst. This result was confirmed by rheological measurements.<sup>2</sup> Plots of heat flow versus time and viscosity versus time for the candidate mixture with and without catalyst to contrast the difference are shown in Figures 10 and 11, respectively. The DSC runs were performed at 130 and 150 °C, whereas the viscosity measurements were performed at 150 and 170 °C.

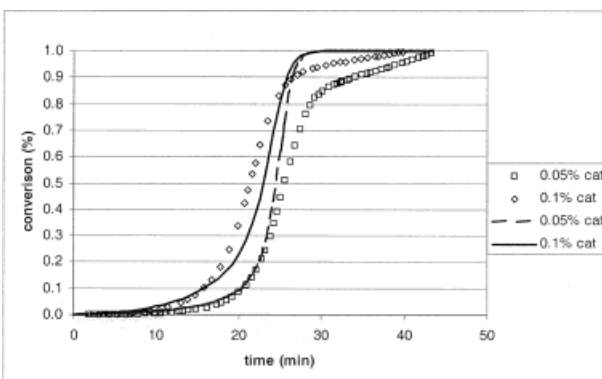


**Figure 9** Dynamic fits (solid lines) to experimental data ( $\diamond$ , 130 °C;  $\square$ , 140 °C;  $\triangle$ , 150 °C).

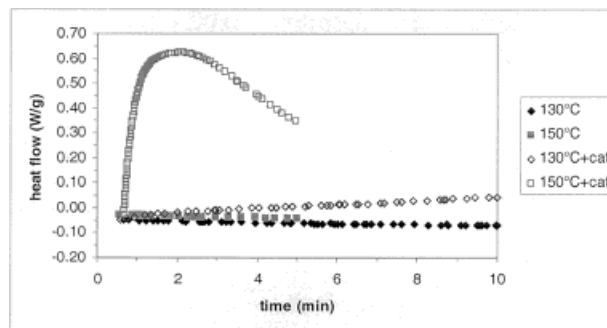


**Figure 10** DSC results show a difference in heat liberation when catalyst is added.

To test if the unreacted mixture displayed shear-thinning behavior, the candidate mixture was prepared without catalyst and run at several temperatures. Data were collected as shear rate was increased from the rate of 1 to  $>100$   $\text{s}^{-1}$ . Shear rates much  $>100$   $\text{s}^{-1}$  gave edge failure. The viscosity of the unreacted mixture was independent of the shear rate. It is difficult to determine if this is the case for the reactive mixture because runs at different shear rates performed as the mixture reacts are confounded with the experimental variability.<sup>10</sup> However, as it will be shown later, the viscosity remains fairly constant up to conversion of 40%. Typical electronic pre-pregs have conversions  $<40\%$  and if some reaction is to be carried out in the pultrusion-type die, it will not reach above this level. Making the assumption of a shear-rate-independent viscosity, or Newtonian behavior, is a good approximation for die design. Near the die end, before the pre-preg reaches the pulling mechanism, the temperature needs to be cooled to a value below the material solidification point (105 °C).

The first order exponential model<sup>12</sup> shown in eq. 7 was used to fit the experimental data at different isothermal temperatures

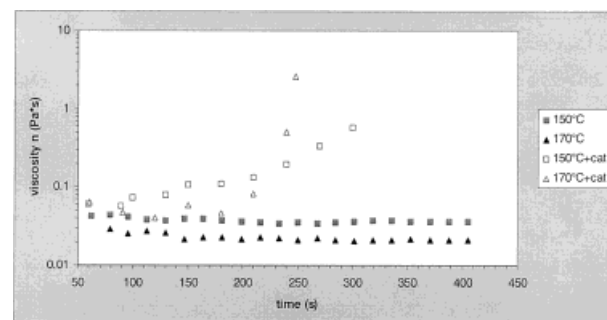


**Figure 11** Viscosity profiles change with the addition of catalyst (2,4-EMI).

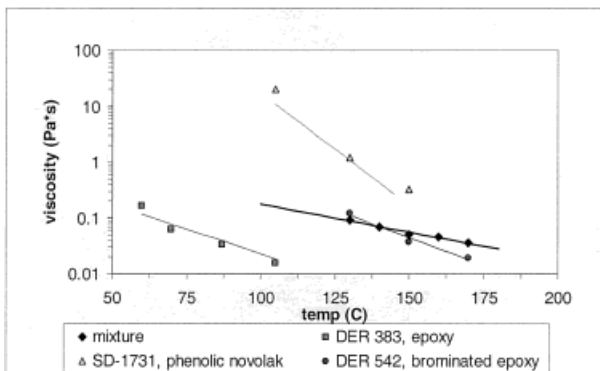


**Figure 12** Viscosity profiles of proposed resin system.

$$\eta = A \cdot e^{-BT} \quad (7)$$

$$A = 979.07 \quad \text{and} \quad B = 0.0231$$

where  $A = 979.07$  and  $B = 0.0231$ . The results are shown in Figure 12, together with the data for the individual resins. The viscosity behavior of the mixture cannot be predicted using the weight or volume average of the viscosities of the individual component.<sup>13</sup> The data were also fit to an Arrhenius expression,<sup>2</sup> but for clarity, only the first-order exponential model is shown.

The effect of fused silica on the viscosity of the candidate system is shown in Figure 13. Fused silica is attractive as a filler because it decreases the dielectric loss and thus improves the signal integrity of the PCB. The results show that the addition of fused silica fillers increases the viscosity but does not change the behavior from Newtonian. Also, no significant change occurs if the filler loading is kept <20% by weight. The experiments shown in Figure 13 were done at 130 °C and the mixture was pre-

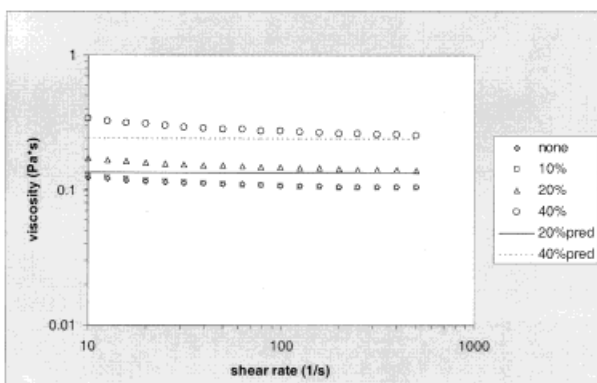


**Figure 13** Effects of filler on viscosity of candidate system at 130 °C.

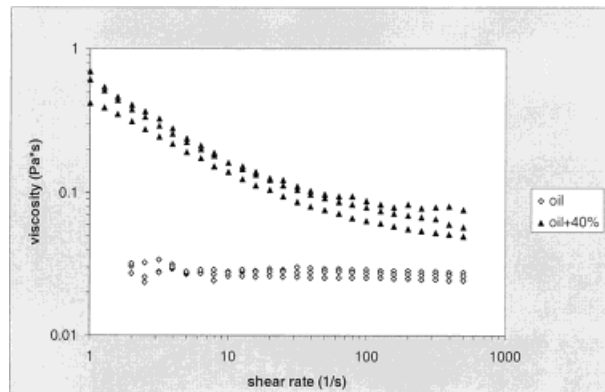


**Figure 14** Shear thinning effect observed with DOP oil and fused silica filler at 30 °C.

pared without catalyst. For reference, the same filler was added to dioctylphthalate (DOP) oil at 30 °C. The results are shown in Figure 14 and resemble what is more typical with the addition of filler; that is, the viscosity not only increases with the addition of filler but the mixture also displays shear thinning behavior. The effects of fillers were fit to a modified Einstein equation, as seen in eq. 8:

$$\eta/\eta_0 = 1 + E\phi^n \quad (8)$$

$$E = 155.39 \quad \text{and} \quad n = 3$$

where  $\eta_0$  is the viscosity of the mixture at the test temperature (130 °C),  $E = 155.39$ , and  $n = 3$ . The predicted values for 20% ( $\phi = 0.109$ ) and 40% ( $\phi = 0.196$ ) fused silica by weight are shown as the lines in Figure 13. This equation does a good job predicting viscosity behavior with added filler.

Isothermal viscosity runs were made at 130, 150, 165, and 175 °C for catalyst levels of 0.05 and 0.1%.<sup>2, 12</sup> As expected, increasing the temperature and catalyst level speeds up the viscosity rise. The viscosity versus time data were converted to viscosity versus conversion<sup>2</sup> using the kinetic expressions presented in the previous section. The results are summarized in Figure 15, where reduced viscosity is plotted versus conversion (reduced viscosity is defined as the viscosity divided by the initial material viscosity). Note that when plotted against the extent of reaction, both catalyst levels merge. However, the reduced viscosity versus extent of reaction did not produce a single curve, so conversion and temperature of the system cannot be decoupled. The data were fit to the



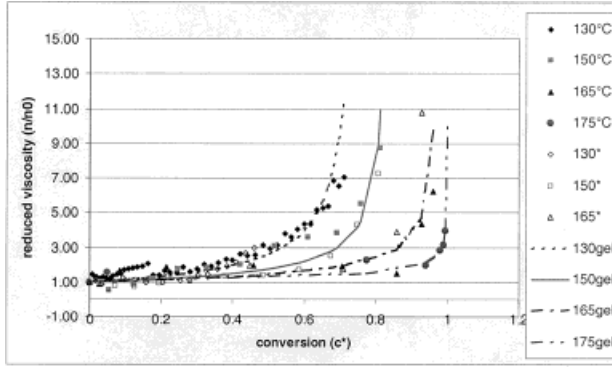


**Figure 15** Gel model (solid line) compared with experimental data (closed symbols are 0.05% catalyst and open symbols are 0.1% catalyst).

gel model as proposed by Halley and Mackay<sup>13</sup> and seen in eq. 9, where  $c_g^*$  is the solidification point:

$$\eta/\eta_0 = (c_g^*/c_g^* - c^*)^B \quad (9)$$

where:

$$c_g^*(T) = -1.5477 + 0.0057 \cdot T \quad (10)$$

$$B(T) = 6.2256 - 0.0132 \cdot T \quad (11)$$

where  $T$  is temperature in K.

The predictions of the model just described are shown as the lines in Figure 15. This model does a good job describing the effect of reaction on the viscosity. Note that the viscosity remains relatively constant until close to the solidification point,  $c_g^*$ , and then rises very sharply at conversions larger than what is desired for typical prepreg to be used in PCB applications.

### Process Windows

In this section, we develop a potential process window for the process using the suggested resin mixture with 0.05% catalyst. Clark-Schwebel 7628 glass fabric will be assumed as the reinforcement material. This glass style is one of the most common used for printed circuit boards. First, consider the impregnation die. Hogade<sup>15</sup> developed an isothermal model to predict the pulling force, as given in eq. 9. This model assumes the development of a lubricating layer on both the top and bottom of the glass fabric as it passes through the die.

$$F/W = 2\eta U(L_1 + L_2)/(h - t) \quad (12)$$

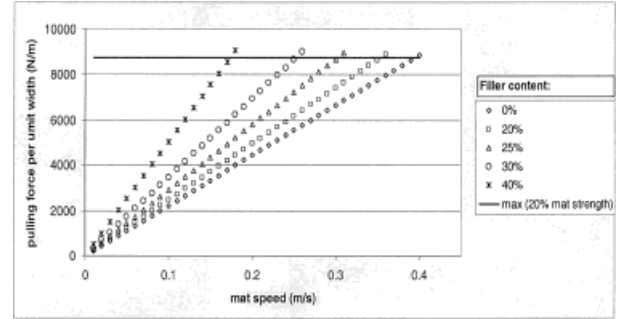


**Figure 16** Process window for mat strength and speed, with varying filler content at 110 °C.

In eq. 12,  $F/W$  is the pulling force per unit width,  $U$  is the mat speed,  $L_1 + L_2$  is the total length of the die, and  $h - t$  is the thickness of the lubricating layer.

Using the chemo-rheology of the candidate resin system, we conclude that if we select the die temperature of 110 °C, no reaction would take place in the die, as discussed previously. This condition would allow the process to run for an indefinite time without the need to stop and clean the die. The resin system should be fed at that temperature. At 110 °C, the material shelf-life is long enough so that on-line mixing may not be needed. Preferably, the glass mat would be preheated to 110 °C prior to entering the die. The viscosity of the mixture at 110 °C is 0.14 Pa\*s, as determined with eq. 7. If 20% filler were added, the viscosity would increase to 0.157 Pa\*s. Using eq. 12 and assuming a die length of 2 m, and a lubricating layer of 0.0000254 m (1 mil), we find that the maximum permissible speed before exceeding 20% of the fabric strength for 7628 (8750 N/m) is 0.35 m/s. Typical maximum line speed for current processes are 0.2 m/s. The process win-

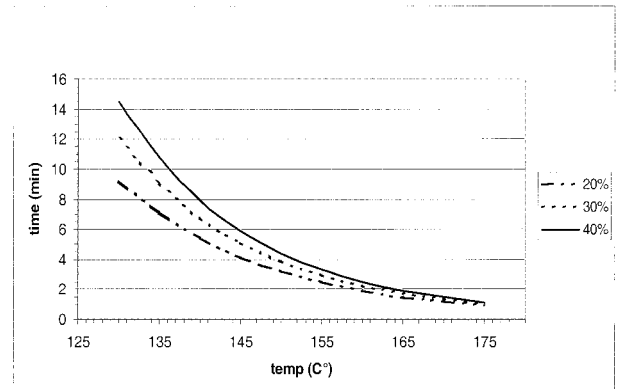


**Figure 17** Residence time needed for several desired pre-preg conversion levels.

dow for the scenario just described at increasing filler levels is shown in Figure 16. As expected, the speed at which the mat can run is slower with increased filler content.

An oven would be located immediately after the die. The residence time required at the indicated temperature for the pre-preg to reach the indicated conversion levels is given in Figure 17. Typical commercial values are between 20 and 40%. Finally, the required residence time in the on-line lamination clamp, assuming that the starting pre-preg conversion is either 20, 30, or 40%, is given in Figure 18. Also, we show the curve for the case where the initial conversion is 0%. In the calculations just described, we assumed that the temperature of the pre-preg remains constant, which is a good approximation because of the small thickness values.

## CONCLUSIONS

A candidate resin system for the proposed solventless process was characterized using chemorheological and kinetic measurements. The equations developed are used to determine important aspects of the process, such as die length, belt clamp length, and maximum allowable mat speed. The main findings in the characterization of the candidate resin system for the proposed solventless process are summarized as follows:

- The candidate resin system does not react appreciably without the addition of catalyst, even at high temperatures.
- The candidate resin system appears to follow two different reaction paths depending on the temperature. According to isothermal DSC runs, one path seems to dominate in the region between 115 and 130 °C, whereas the second dominates at >130 °C.
- The candidate resin system displayed no reaction, even with the addition of catalyst, at 110 °C. This information is very useful when considering the design of the pultrusion-type die and B-staging oven. Because the resin will not react at 110 °C, the die could be kept at that temperature to allow impregnation, and the partial curing could take place in another oven.
- Three factors affect the viscosity of the system: temperature, filler content, and conversion. A general set of equations was obtained to aid in determining processing windows. The model does a good job predicting chemo-

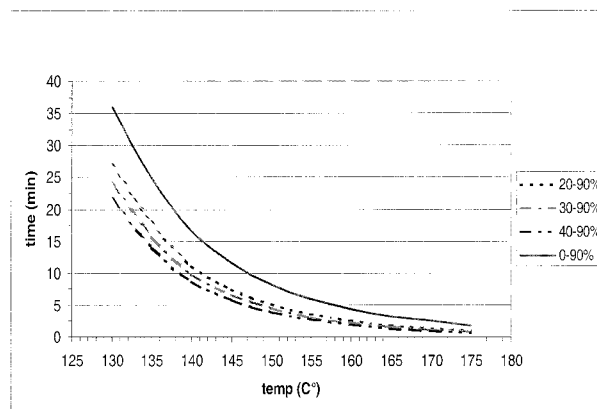


**Figure 18** Residence time needed to cure in the belt clamp at several starting conversion levels.

rheological changes in the processing temperature range 110–175 °C.

The authors thank the National Science Foundation for funding this research (grant £DMI-9900121), Dow Chemical, and Allied Signal for experimental materials and technical advice.

## REFERENCES

1. Shirrell, C. D.; Christiansen, W. H.; Iyer, S.; Brave-nec, L. D. IPC Proceedings, 1996.
2. Dehnke, L. M. M.S. Thesis, The Ohio State University, 2000.
3. Lee, H.; Neville, K. Handbook of Epoxy Resins; McGraw: New York, 1976.
4. Theriault, R. P.; Osswald, T.A.; Castro, J. M. Polym Com 1999, 20, 493.
5. Colucci, M. J. M.S. Thesis, University of Texas – Austin, 1984.
6. Khomu, S.; Khomami, B.; Kardos, J. Polym Com 1998, 19, 335.
7. Din, Z.; Li, S.; Lee, L. J.; Engled, H.; Puckett, M.; Polym Comp Oct, 2000.
8. Kamal, M. R.; Sorour, S. Polym Eng Sci 1973, 13, 59.
9. Gonzalez, V.M., Ph. D. Thesis, University of Minnesota, Minneapolis, MN, 1983.
10. Castro, J. M.; Perry, S. J.; Macosko, C.W. Polym Com 1984, 25, 82.
11. Li, M. M.S. Thesis, The Ohio State University, 2000.
12. Castro, J. M.; Macosko, C. W. A J Chem Eng J 1982, 28, 250.
13. Dehnke, L. M.; Castro, J. M.; Li, M.; Lee, L. J.; Proceedings from Antec 2000.
14. Halley, P. J.; MacKay, M. E. Poly Eng Sci 1996, 36, 593.
15. Hogade, R. R. M.S. Thesis, The Ohio State University, 2000.